NASA TECHNICAL NOTE

NASA TN D-4346

NASA TN D-4346

DUCTILITY MECHANISMS AND SUPERPLASTICITY IN CHROMIUM ALLOYS

by Joseph R. Stephens and William D. Klopp

Lewis Research Center
Cleveland, Ohio

NATIONAL AERONAUTICS AND SPACE ADMINISTRATION • WASHINGTON, D. C. • JANUARY 1968

DUCTILITY MECHANISMS AND SUPERPLASTICITY IN CHROMIUM ALLOYS

By Joseph R. Stephens and William D. Klopp

Lewis Research Center
Cleveland, Ohio

NATIONAL AERONAUTICS AND SPACE ADMINISTRATION

For sale by the Clearinghouse for Federal Scientific and Technical Information
Springfield, Virginia 22151 – CFSTI price $3.00

DUCTILITY MECHANISMS AND SUPERPLASTICITY IN CHROMIUM ALLOYS

by Joseph R. Stephens and William D. Klopp

Lewis Research Center

SUMMARY

A study was conducted to identify and characterize chromium alloys exhibiting good low-temperature ductility. Alloys with lower ductile-to-brittle transition temperatures than that of unalloyed chromium (~300° F or 422° K) included chromium - 35 to 40 atom percent rhenium, chromium - 15 to 24 atom percent ruthenium, chromium - 30 atom percent cobalt, and chromium - 30 to 50 atom percent iron. Equilibrium diagrams for these four systems have two features in common, an intermediate σ phase and a high maximum solubility of solute in chromium. Alloys from systems that did not have both of these features were either unfabricable or had transition temperatures greater than that of unalloyed chromium.

The following observations were made on alloys with compositions approaching the solubility limit in the chromium-rhenium, chromium-ruthenium, and chromium-cobalt systems and the σ composition in the chromium-iron system: ductile-to-brittle transition temperature decreased significantly; grain size increased sharply with increasing solute content after annealing at a constant temperature; hardness decreased substantially; and initial deformation was primarily by twinning.

Additionally, the ductile-to-brittle transition temperatures of near saturated alloys can be related to the fractional difference in specific volume between the σ phase and the respective chromium-base solid solution.

Chromium - 30 atom percent cobalt and chromium - 24 atom percent ruthenium alloys were tensile tested at elevated temperatures and exhibited superplasticity characterized by high, neck-free elongations. Observation of superplasticity in two of the alloy systems investigated suggests the rhenium ductilizing effect and superplasticity may have common basic features.

INTRODUCTION

Chromium (Cr) alloys are currently being investigated for advanced air-breathing engine applications, primarily as turbine buckets and/or stator vanes. The inherent advantages of Cr as a high-temperature structural material are well known (ref. 1) and include its high melting point relative to superalloys, moderately high modulus of elasticity, low density, good thermal shock resistance, and superior oxidation resistance as compared to the other refractory metals. Additionally, it is capable of being strengthened by conventional alloying techniques.

The major disadvantage of Cr is its poor ductility at ambient temperatures, a problem which it shares with the other two Group VI-A metals, molybdenum (Mo) and tungsten (W). For Cr, the problem is further amplified by its susceptibility to nitrogen (N) embrittlement during high-temperature air exposure. (In cases of severe nitrogen embrittlement, the ductile-to-brittle transition temperature might even exceed the steady-state operating temperature of the component.) The low ductility of Cr would make stator vanes and turbine buckets prone to foreign object damage during engine startup when these components are cold.

The present work was directed towards improvement of the inherent ductility of Cr through alloying, with the anticipation that any improvements so obtained might be additive to strengthening improvements achieved through different types of alloying. The alloying additions for ductility were selected on two bases:

(1) Elements which might lower the hardness of Cr at low alloying levels

(2) Elements with phase relations to Cr similar to that of chromium-rhenium (Cr-Re).

Hardness minima have been observed in numerous Cr alloys containing small additions of the Group IV-A to VIII elements. These minima have been tentatively attributed to reduced interstitial solubilities in Cr (ref. 2). Improvements in the ductility of cast Cr by dilute alloying have also been observed (ref. 3), but not in wrought Cr. However, a reduction in the hardness of W by dilute Re additions has recently been shown to be accompanied by improved cold ductility in both wire (ref. 4) and sheet (ref. 5), which gives some indication that similar behavior might be found in Cr.

Dilute alloy additions evaluated in the present study were vanadium (V), manganese (Mn), rhenium (Re), iron (Fe), ruthenium (Ru), osmium (Os), iridium (Ir), and yttrium (Y). The properties evaluated included hardness, fabricability, and ductile-to-brittle bend-transition temperature.

The reduction in the ductile-to-brittle transition temperatures of the Group VI-A metals as a result of alloying with 25 to 35 atomic percent Re is well established (refs. 6 to 8). These alloys typically deform initially by twinning at low temperatures. This phenomenon is commonly referred to as the Re ductilizing effect. This terminology

is also used to describe systems in which the ductilizing element is not Re. Other alloy systems which have recently been shown to exhibit the rhenium ductilizing effect include chromium-cobalt (Cr-Co) and chromium-ruthenium (Cr-Ru) (see ref. 9).

In order to explore the generality of this effect, alloys were selected from systems having phase relations similar to that of chromium-rhenium (Cr-Re), primarily a high solubility in Cr and an intermediate σ phase. In addition to Cr-Re, four other systems were evaluated which have these features: Cr-Ru, Cr-Co, chromium-iron (Cr-Fe), and chromium-manganese (Cr-Mn).

Seven other systems were also studied which partially resemble Cr-Re. These systems have extensive Cr solid solutions or a complex intermediate phase not necessarily σ; these are chromium-titanium (Cr-Ti), chromium-vanadium (Cr-V), chromium-columbium (Cr-Cb), chromium-tantalum (Cr-Ta), chromium-nickel (Cr-Ni), chromium-osmium (Cr-Os), and chromium-iridium (Cr-Ir).

The compositions of alloys in these systems were chosen near the solubility limit for the Cr-base solid solutions. (In the Group VI-A Re systems, the saturated alloys are the most ductile.) These alloys were evaluated on the bases of hardness, fabricability, and ductile-to-brittle transition temperatures.

In addition to the studies of alloying effects on ductility, a minor investigation was conducted on superplasticity at high temperatures in Cr-Co and Cr-Ru alloys. (This study on Cr-Co is also reported in ref. 10).

EXPERIMENTAL PROCEDURE

Melting and Fabrication

High-purity Cr prepared by the iodide (I) deposition process was employed for all studies. An analysis of this Cr is given in table I.

TABLE I. - ANALYSIS OF IODIDE CHROMIUM

Element												
Al	Co	Cu	Fe	Mg	Mn	Ni	Si	V	C	H	N	O
Impurity content, ppm by weight												
1.0	2.0	0.1	11.0	2.0	0.1	1.0	10.0	1.0	10.0	0.3	1.9	2.0

Alloy elements were obtained in the forms given below:

Cb	electron-beam-melted sheet
Co	electrolytic flake; electron-beam-melted ingot
Fe	electrolytic flake
Ir	commercially pure powder
Mn	electrolytic flake
Mo	commercially pure powder
Ni	electrolytic flake
Os	commercially pure powder
Re	commercially pure powder; arc-melted sheet
Ru	commerically pure powder
Ta	electron-beam melted sheet
Ti	arc-melted ingot
V	arc-melted ingot
W	commercially pure powder
Y	arc-melted ingot

Most alloys were prepared from mixtures of Cr and the elemental alloy additions. Master alloys of Cr-25Ir, Cr-30Re, Cr-40Re, and Cr-20Ru were also employed to reduce inhomogenieties in the final alloys.

All alloys were initially consolidated by triple arc-melting into 60-gram button ingots on a water-cooled copper (Cu) hearth using a nonconsumable W electrode. The melting atmosphere was Ti-gettered argon (Ar) at a pressure of 20 torr (26.6×10^2 N/m^2).

Three methods of fabrication to 0.035 inch (0.9 mm) sheet were employed:

(1) Direct rolling of the arc-melted buttons

(2) Press forging of the arc-melted buttons followed by rolling

(3) Drop casting the ingots into rectangular slabs followed by rolling

The last method appeared to give best results and was employed for the majority of the alloys. Cladding in mild steel was also used to facilitate fabrication. Rolling temperatures ranged from 1472° to 2800° F (1073° to 1811° K).

Specimen Preparation

Bend specimens measuring 0.3 by 0.9 inch (7.6 by 22.9 mm) were cut from the 0.035 inch (0.9 mm) rolled sheet parallel to the rolling direction. Surface oxide formed during rolling was removed by machine grinding or low-pressure sand blasting. The bend specimens were sealed in Vycor under Ar and annealed at a constant temperature for each alloy system to give an equiaxed, single-phase structure prior to testing. The specimens were either furnace cooled or water quenched, followed by electropolishing in a solution of 30 milliliters of 70 percent perchloric acid and 70 milliliters of acetic acid at 10 volts.

Figure 1 shows the design of tensile specimens used for this study. Blanks measuring 3/4 by 3 inch (19 by 76 mm) were cut from the sheet and ground to a uniform thickness. The gage section and grip holes were cut by electrical discharge machining. Specimens were electropolished prior to tensile testing.

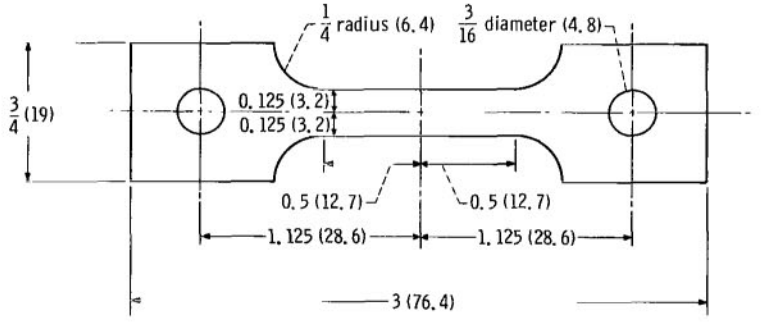

Figure 1. - Tensile specimen design. All dimensions given in inches (millimeters).

Bend Testing

Bend tests were conducted at a crosshead speed of 1 inch (25 mm) per minute over a bend radius approximately four times the specimen thickness (4T). Steel rollers were used for both the plunger and the two support pins, which were positioned at a span of 0.75 inch (19 mm). The bend apparatus is described in detail in reference 11. A controlled liquid nitrogen (N) spray was used to achieve test temperatures below room temperature. Tests above room temperature were conducted in air in a quartz tube radiation furnace. Temperature was measured by a thermocouple in contact with the loading fixture adjacent to the test specimen. The bend-transition temperature is defined as the lowest temperature at which a specimen could be bent 100^{o}, the limit of the bend fixture.

Tensile Testing

Elevated temperature tensile tests were conducted in an Ar atmosphere at a crosshead speed of 0.01 inch per minute (0.25 mm/min). Two platinum - platinum-13-percent-rhodium (Pt - Pt-13-percent-Rh) thermocouples were used to measure temperature. One thermocouple was located at the center of the gage section and the second at the top of the gage section, 0.5 inch (12.7 mm) above the first. Temperature difference between the two couples did not exceed 20 F^{o} (11 K^{o}) at the start of testing. Specimens were annealed in situ at temperature for 1 hour and then held at the test temperature for 5 minutes prior to initiation of the test. Stress was calculated from the load-time recording on the testing machine and the original cross-sectional area of the specimens. Elongation was determined by measuring the distance between gage marks on the specimen before and after testing.

Hardness and Metallographic Examination

Vickers hardness was determined for as-cast alloys using a 10-kilogram load. Microhardness was also measured on metallographic specimens using a 1-kilogram load and a micro-Vickers indentor.

Specimens were examined metallographically after bend testing to determine grain size and hardness, and to study the deformation mechanisms.

Elevated Temperature X-ray Diffraction

The effects of V, Cb, Ta, Mo, and W on the solvus temperature of Cr-30Co[1] were investigated by elevated temperature X-ray diffraction. Arc-melted specimens were ground to -320 mesh powder which was placed on the Ta heater of an X-ray diffraction furnace and heated in a helium (He) atmosphere. Approximate solvus temperatures for the ternary alloys were determined by monitoring σ lines as the specimens were heated. Disappearance of the σ lines was the criterion used to indicate the solvus temperature. A thermocouple attached to the heater provided accurate temperature measurements.

---

[1]Alloy compositions are in atomic percent unless otherwise stated.

RESULTS AND DISCUSSION

Dilute Chromium-Base Alloys

Binary alloys of Cr with 0.1 to 10 atomic percent Re, Ru, and Ir, 0.3 to 1.0 atomic percent Os, Mn, and Fe, and 0.1 to 3.0 atomic percent V were melted and drop cast into

TABLE II. - FABRICATION OF CHROMIUM AND DILUTE CHROMIUM BASE ALLOYS

Nominal composition, at. %	As-cast hardness for 10-kg load, VHN	Rolling temperature, °F	Rolling temperature, °K	Reduction in thickness, percent	Condition after rolling
		Unalloyed chromium			
100Cr[a]	128	1472	1073	89	Good
100Cr[a]	127	1472	1073	89	
100Cr[a]	131	1472	1073	90	
100Cr	127	1500	1089	94	
		Cr-Re			
Cr-0.1 Re[b]	107	1500	1089	93	Fair
Cr-0.2 Re[c]	---	1600	1144	43	Cracked
Cr-0.3 Re[b]	111	2000	1366	0	Cracked first pass
Cr-0.4 Re[c]	---	1600	1144	92	Cracked
Cr-0.5 Re[b]	116	1500	1089	93	Fair
Cr-0.6 Re[c]	---	1600	1144	[d]93	Cracked
Cr-1.0 Re[b]	121	1500	1089	93	Fair
Cr-1.0 Re[c]	---	1600	1144	[d]93	Fair
Cr-3.0 Re[c]	153	1900	1311	0	Cracked first pass
Cr-5.0 Re[c]	196	1500	1089	0	Cracked first pass
Cr-10.0 Re[c]	244	1700	1200	0	Cracked first pass
		Cr-Ru			
Cr-0.1 Ru[e]	105	1600	1144	93	Good
Cr-0.2 Ru	---			[d]93	Fair
Cr-0.4 Ru	---			92	Fair
Cr-0.5 Ru[e]	115			93	Good
Cr-0.6 Ru	---			[d]93	Good
Cr-1.0 Ru	---			93	Good
Cr-3.0 Ru[e]	193			76	Cracked
Cr-10.0 Ru[e]	335			89	Good
		Cr-Ir			
Cr-0.1 Ir[f]	100	1600	1141	93	Cracked
Cr-0.2 Ir	---			[d]93	Good
Cr-0.4 Ir	---			[d]90	Fair
Cr-0.5 Ir[f]	130			93	Fair
Cr-0.6 Ir	---			[d]86	Cracked
Cr-1.0 Ir	---			[d]92	Good
Cr-3.0 Ir[f]	250			0	Cracked first pass
Cr-10.0 Ir[f]	395			93	Fair
		Cr-Os			
Cr-0.3 Os	144	1700	1200	0	Cracked first pass
Cr-0.6 Os	146	1700	1200	0	Cracked first pass
Cr-1.0 Os	162	1700	1200	0	Cracked first pass
		Cr-Mn			
Cr-0.3 Mn	118	1700	1200	92	Good
Cr-0.6 Mn	108	1700	1200	95	Good
Cr-1.0 Mn	121	1700	1200	92	Good
		Cr-Fe			
Cr-0.3 Fe	149	1700	1200	0	Cracked first pass
Cr-0.6 Fe	153	1700	1200	0	Cracked first pass
Cr-1.0 Fe	167	1700	1200	0	Cracked first pass
		Cr-V			
Cr-0.5 V	148	1700	1200	[d]92	Fair
Cr-1.0 V	149			[d]80	Cracked
Cr-1.5 V	156			[d]76	Cracked
Cr-2.0 V	163			[d]94	Fair
Cr-2.5 V	164			[d]92	Fair
Cr-3.0 V	186			[d]92	Cracked
		Cr-Y			
Cr-0.1 Y	150	1550	1116	92	Good
		Cr-Y-Re			
Cr-0.1 Y-0.1 Re	---	1550	1116	92	Good
Cr-0.3-0.1 Re	144	1600	1144	92	
Cr-0.5-0.1 Re	---	1600	1144	89	
Cr-1.0-0.1 Re	260	1600	1144	92	

[a]Cast button fabricated directly; other buttons were drop cast to slab form before fabricating.
[b]Prepared from master alloy of Cr-40Re or Cr-30Re.
[c]Rhenium added as sheet rolled from arc-melted button.
[d]Canned in steel or molybdenum during rolling.
[e]Prepared from master alloy of Cr-20Ru.
[f]Prepared from master alloy of Cr-25Ir.

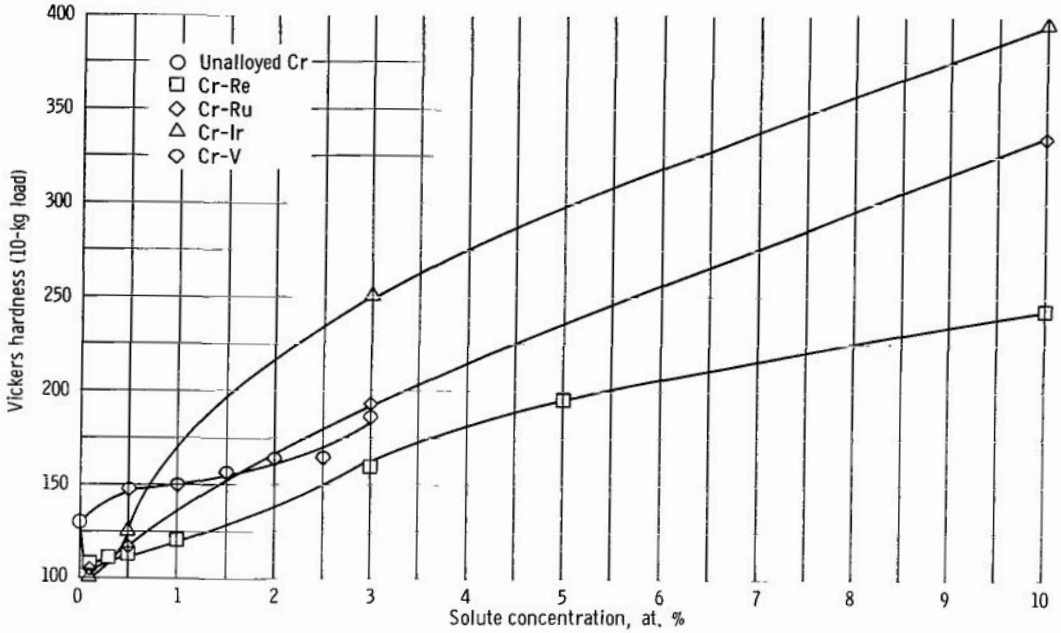

Figure 2. - Room-temperature hardness of as-cast Cr alloys with a maximum of 3.0 to 10.0 atomic percent solute.

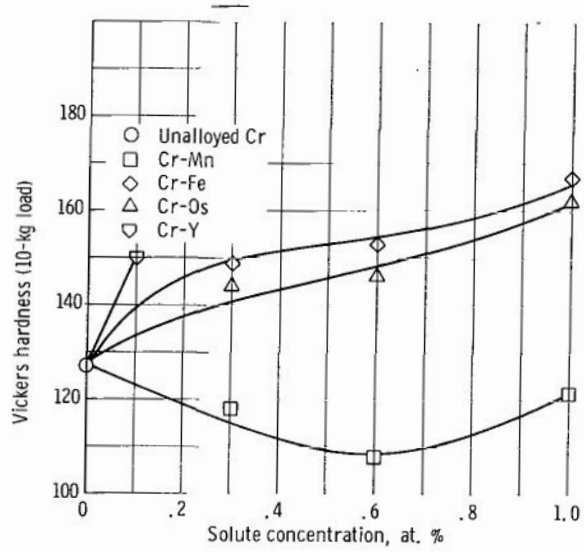

Figure 3. - Room-temperature hardness of as-cast Cr alloys with a maximum of 1.0 atomic percent solute.

rectangular ingots. Fabrication history and as-cast hardness of these alloys are presented in table II and the hardnesses are shown in figures 2 and 3.

Dilute additions of Re, Ru, Ir, and Mn decreased the hardness of Cr, while V, Fe, and Os effected a moderate increase in hardness. These results are in agreement with previously reported results (ref. 2) except for the V, Fe, and Os additions.

As shown in table II, fabrication of many of these alloys was either unsuccessful or difficult. Ductile-to-brittle bend-transition temperatures were determined for the few fabricable alloys and in all cases were higher than the 300° F (422° K) transition tem-

TABLE III. - MICROHARDNESS, GRAIN SIZE, AND BEND-TRANSITION TEMPERATURES FOR CHROMIUM AND CHROMIUM ALLOYS

Nominal composition, at. %	Annealing temperature[a]		Microhardness for 1-kg load, VHN	Grain size, mm	Ductile-to-brittle bend-transition temperature			
					Furnace cooled		Quenched	
	°F	°K			°F	°K	°F	°K
Unalloyed chromium								
100Cr	2000	1366	127	0.045	300	422	300	422
Binary alloys - dilute								
Cr-1Re	2400	1589	---	-----	----	----	400	478
Cr-0.1 Ru	2200	1478	105	-----	----	----	500	533
Cr-0.2 Ru	↓	↓	---	-----	----	----	750	672
Cr-0.5 Ru			115	-----	----	----	300	422
Cr-0.6 Ru			---	-----	----	----	850	728
Cr-10.0 Ru			---	-----	----	----	800	700
Cr-0.4 Ir	2000	1366	---	-----	----	----	700	644
Cr-10.0 Ir	2500	1644	---	-----	----	----	>500	>533
Cr-0.3 Mn	2000	1366	---	-----	----	----	450	505
Cr-0.6 Mn	2000	1366	---	-----	----	----	650	616
Cr-1.0 Mn	2000	1366	---	-----	----	----	>700	>644
Cr-0.1 Y	2400	1589	150	-----	150	339	150	339
Binary alloys - concentrated								
Cr-35Re	2400	1589	326	0.017	-200	144	-300	89
Cr-40Re	2400	1589	339	.023	----	----	-300	89
Cr-15Ru	2200	1478	422	.031	250	394	200	366
Cr-18Ru	↓	↓	406	.029	100	311	25	269
Cr-21Ru			396	.039	-200	144	-175	158
Cr-24Ru			392	.132	----	----	-250	116
Cr-27Ru			421	.207	----	----	-150	172
Cr-25Co	2350	1561	574	.104	>900	>755	700	644
Cr-30Co	2350	1561	528	.294	700	644	-200	144
Cr-30Fe	2300	1533	361	.029	450	505	300	422
Cr-40Fe	2300	1533	314	.153	400	478	200	366
Cr-50Fe	2300	1533	254	.171	250	366	-75	214
Cr-12Os	3000	[b]1922	281	.104	----	----	700	644
Cr-15Os	3000	[b]1922	298	.180	----	----	600	589
Ternary alloys - dilute								
Cr-0.1 Y-0.1 Re	2400	1589	---	-----	----	----	300	422
Cr-0.1 Y-0.3 Re	↓	↓	144	-----	250	394	250	394
Cr-0.1 Y-0.5 Re			---	-----	----	----	250	394
Cr-0.1 Y-1.0 Re			260	-----	350	450	350	450
Ternary alloy - concentrated								
Cr-0.8 Re-20Co	2350	1561	---	-----	----	----	800	700
Cr-0.8 Re-25Co	↓	↓	---	-----	----	----	500	533
Cr-0.1 Re-30Co			---	-----	>900	>755	----	----
Cr-0.3 Re-30Co			---	-----	----	----	----	----
Cr-0.8 Re-30Co			---	-----	----	----	375	464
Cr-3.0 Re-30Co			---	-----	----	----	800	700

[a]Specimens annealed 1 hr at indicated temperatures and water quenched or furnace cooled.
[b]Quenched by withdrawing from hot zone of furnace and flowing argon over specimens.

perature for unalloyed Cr. These results are tabulated in table III.

Dilute Y additions to Cr have been reported to not only improve the oxidation and nitridation resistance of Cr, but also to reduce the ductile-to-brittle transition temperature (ref. 12). In the present program, the addition of 0.1 atomic percent Y reduced the transition temperature from 300° to 150° F (422° to 339° K), although the hardness increased from 127 to 150 Vicker's hardness number, figure 3.

Ternary alloys were melted to determine if a combination of Y gettering and Re softening would further lower the transition temperature. However, the ternary alloys had transition temperatures higher than that of the Cr-0.1Y binary alloy, as listed in table III and shown in figure 4.

Thus, it must be concluded from these results that dilute solid solution alloying with elements which decrease the hardness of Cr is ineffective in improving the ductility of wrought and annealed Cr. Yttrium, which increases the hardness and probably acts primarily as a scavenger for interstitials, appears unique in significantly improving the ductility of wrought Cr as a dilute addition.

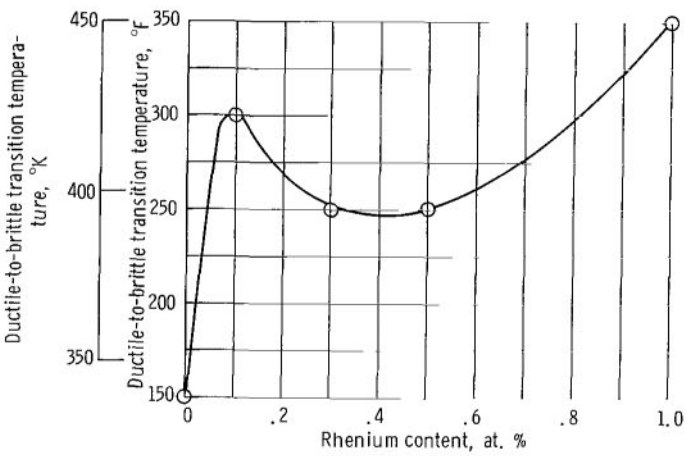

Figure 4. - Effect of rhenium content on ductile-to-brittle transition temperatures for Cr-0.1Y alloys. Annealed hour at 2400° F (1589° K); water quenched.

CONCENTRATED CHROMIUM-BASE ALLOYS

Heat Treatments

The equilibrium diagrams for the Cr-Re, Cr-Ru, Cr-Fe, and Cr-Co alloy systems are shown in figure 5 (refs. 13 to 15). These systems have two features in common: the solute has a high solubility in Cr, ranging from approximately 30 atomic percent for Ru up to complete solubility for Fe in Cr, and each of the alloy systems contains an intermediate σ phase having a narrow-composition range. The σ structure is tetragonal with

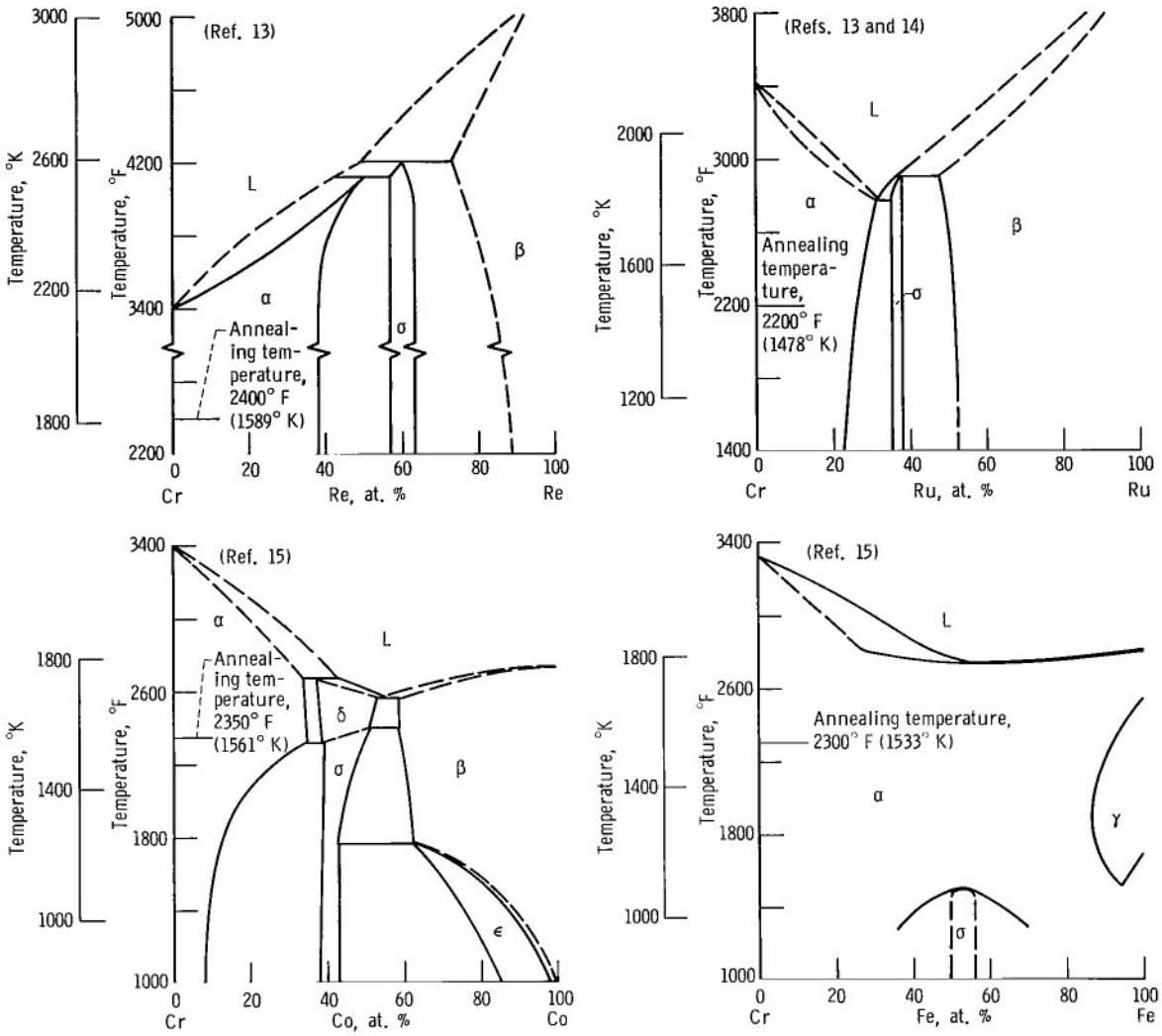

Figure 5. - Equilibrium phase diagrams for primary Cr alloy systems investigated.

a c/a ratio of approximately 0.5, and contains 30 atoms per unit cell (ref. 16). The Cr-Mn system (not shown) also has similar features.

Alloys from these five systems and seven others (which show partial resemblance to Cr-Re system), Cr-Ti, Cr-V, Cr-Cb, Cr-Ta, Cr-Os, Cr-Ni, and Cr-Ir, were arc-melted and fabricated as shown in table IV. Good sheet was obtained from alloys in five systems (Cr-Co, Cr-Re, Cr-Ru, Cr-Os, and Cr-Fe), while all alloys studied from the other seven systems could not be fabricated.

Bend specimens were cut from the fabricable strips and annealed to a recrystalized, equiaxed structure before bend testing. A constant annealing temperature was employed for each alloy system. The temperature selections were based partially on the phase diagram to ensure that the alloys were single phase during annealing and are indicated in

TABLE IV. - FABRICATION OF CHROMIUM AND CONCENTRATED CHROMIUM ALLOYS

Nominal composition, at. %	As-cast hardness for 10-kg load, VHN	Rolling temperature, °F	Rolling temperature, °K	Reduction in thickness, percent	Condition after rolling
Cr-Re					
Cr-25Re	325	1472	1073	[a]30	Cracked
Cr-30Re	390	1832	1273	[a]75	Cracked
Cr-35Re	397	1832	1273	[a]71	Fair
Cr-35Re[b]	---	2375	1575	[c]83	Fair
Cr-35Re[b]	393	2375	1575	[c]89	Good
Cr-35Re	393	2400	1589	94	Fair
Cr-40Re	---	----	----	[c]---	Forging unsuccessful
Cr-40Re[b]	323	2400	1589	[a]92	Good
Cr-Ru					
Cr-15Ru	422	1850	1283	93	Good
Cr-18Ru	406	↓	↓	↓	↓
Cr-18Ru	---				
Cr-18Ru	---				
Cr-21Ru	396			92	
Cr-21Ru	---	2300	1533	93	
Cr-21Ru	---	2300	1533	↓	
Cr-24Ru	392	2100	1432		
Cr-24Ru	---	↓	↓		
Cr-24Ru	---				
Cr-24Ru	---				
Cr-27Ru	---	2300	1533		
Cr-27Ru	---	2300	1533	↓	
Cr-30Ru	---	2100	1422	0	Cracked first pass
Cr-30Ru	---	2300	1533	91	Cracked
Cr-Co					
Cr-20Co[d]	539	2012	1373	[a]90	Good
Cr-20Co	575	2350	1561	93	↓
Cr-25Co[d]	572	2012	1373	[a]90	
Cr-25Co	574	2350	1561	93	
Cr-30Co[d]	850	2012	1373	[a]90	
Cr-30Co[d]	---	2012	1373	[a]0	Cracked first pass
Cr-30Co[d]	780	2375	1575	87	Poor
Cr-30Co[d]	---	2012	1373	[a]64	Severe cracking
Cr-30Co[d]	573	2400	1589	93	Good
Cr-30Co	528	2350	1561	94	↓
Cr-30Co	---	↓	↓	93	
Cr-30Co	---			93	
Cr-30Co	---			93	↓
Cr-Fe					
Cr-30Fe	361	1500	1089	93	Good
Cr-40Fe	314	1600	1144	93	Good
Cr-50Fe	254	1600	1144	93	Good

Nominal composition, at. %	As-cast hardness for 10-kg load, VHN	Rolling temperature, °F	Rolling temperature, °K	Reduction in thickness, percent	Condition after rolling
Cr-Os					
Cr-6Os	317	2400	1589	40	Cracked
Cr-9Os	279	↓	↓	27	Cracked
Cr-12Os	281			93	Good
Cr-15Os	298			93	Good
Cr-Mn					
Cr-35Mn	340	2400	1589	0	Cracked first pass
Cr-45Mn	325	2400	1589	0	Cracked first pass
Cr-55Mn	301	2200	1478	89	Fair
Cr-65Mn	224	2100	1422	92	Fair
Cr-Ta					
Cr-0.6 Ta	---	2400	1589	[e]0	Cracked first pass
Cr-1.2 Ta	---	2400	1589	[e]0	Cracked first pass
Cr-2.4 Ta	---	2400	1589	[e]0	Cracked first pass
Cr-2.5 Ta	---	2800	1811	21	Cracked
Cr-V					
Cr-15V	---	2000	1366	0	Cracked first pass
Cr-30V	---	2200	1478	0	Cracked first pass
Cr-45V	---	2400	1589	0	Cracked first pass
Miscellaneous binary alloys					
Cr-20Ni	---	2400	1589	78	Cracked
Cr-20Ti	---	2800	1811	0	Cracked first pass
Cr-2.5 Cb	---	2400	1589	0	Cracked first pass
Cr-Re-Co					
Cr-0.8 Re-20Co	---	2400	1589	92	Edge cracks
Cr-0.8 Re-25Co	---	↓	↓	↓	Edge cracks
Cr-0.1 Re-30Co	572				Good
Cr-0.3 Re-30Co	545				Good
Cr-0.3 Re-30Co	578				Good
Cr-0.8 Re-30Co	533				Edge cracks
Cr-30Re-5Co	---	↓	↓	0	Cracked first pass
Cr-10Re-10Co	---	2300	1533	32	Cracked
Cr-25Re-10Co	---	↓	↓	0	Cracked first pass
Cr-12Re-12Co	---			35	Cracked
Cr-14Re-14Co	---			30	Cracked
Cr-25Re-15Co	---			0	Cracked first pass
Cr-16Re-16Co	---	↓	↓	18	Cracked

[a]Cast button fabricated directly; other buttons were drop cast to slab form before fabricating.

[b]Rhenium added as sheet rolled from arc-melted button.

[c]Forged at 2400° F (1589° K) to ~70-percent reduction; rolled at room temperature for final reduction.

[d]Prepared from electrolytic cobalt; electron-beam-melted cobalt added to other alloys.

[e]Extruded at 2800° F (1181° K) to ~80-percent reduction prior to rolling.

figure 5 and table IV. The specimens were either water quenched or furnace cooled from the annealing temperature prior to testing.

Metallography

The four alloy systems on which most work was done (Cr-Re, Cr-Ru, Cr-Co, and Cr-Fe) can be separated into two categories based on the temperature dependence of the solubility limit, that is, the slope of the solvus line in the phase diagram. Those systems whose solubility limits of the solute in Cr are relatively insensitive to temperature include Cr-Ru and Cr-Re. In the second category, which includes Cr-Fe and Cr-Co, the solubility limits are highly temperature dependent. Metallographic examination revealed that the σ phase did not precipitate after either quenching or furnace cooling from annealing temperatures of 2200° F (1478° K) for Cr-Ru and 2400° F (1589° K) for Cr-Re. This is illustrated in figure 6 for a Cr-35Re alloy.

Quenching from the solution annealing temperatures of 2300° F (1533° K) and 2350° F (1561° K) for Cr-Fe and Cr-Co, respectively, prevented precipitation of σ, as shown in figure 7(a) for the Cr-30Co alloy. Furnace cooling resulted in precipitation of σ in the

(a) One hour at 2400° F (1589° K), quenched. (b) One hour at 2400° F (1589° K), furnace cooled.

Figure 6. - Comparison of microstructures of Cr-35Re (at. %) as function of cooling rate from annealing temperature. X250.

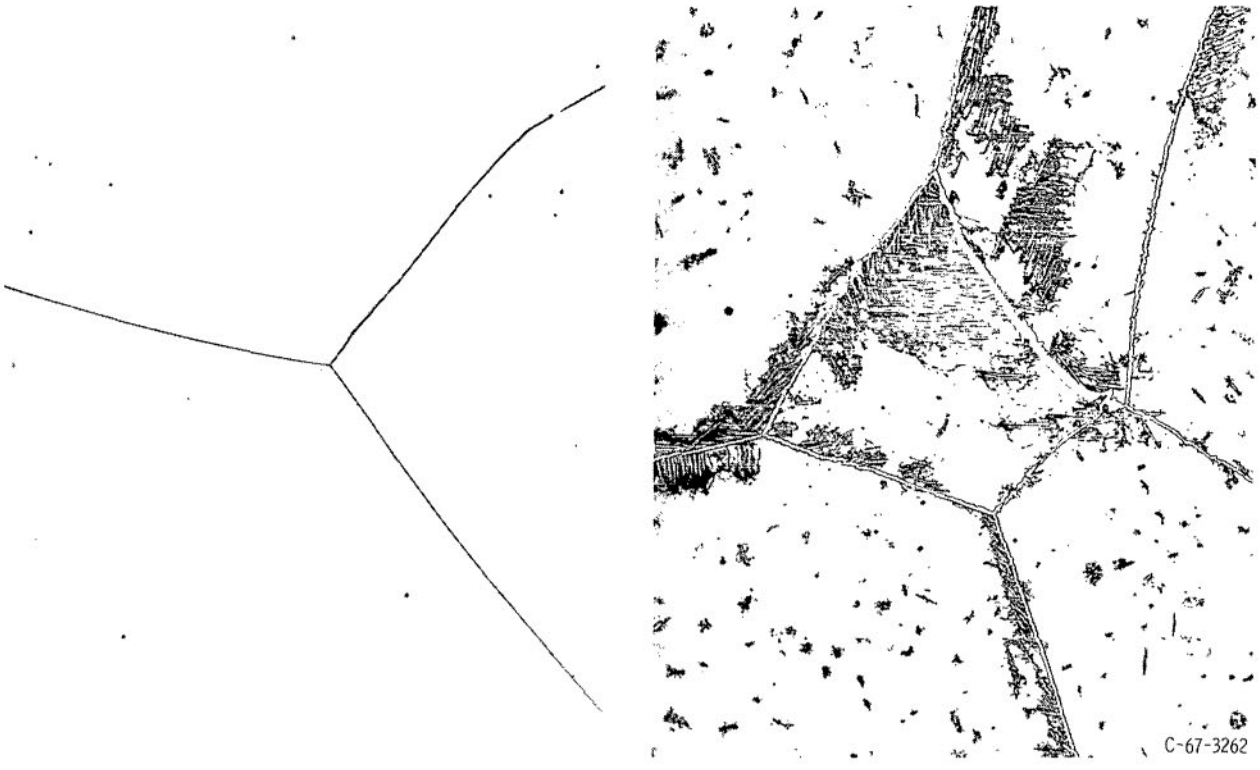

(a) One hour at 2350° F (1561° K), quenched.

(b) One hour at 2350° F (1561° K), furnace cooled.

Figure 7. - Comparison of microstructures of Cr-30Co (at. %) as function of cooling rate from annealing temperature. X250.

Cr-Co and Cr-Fe alloys and as illustrated in figure 7(b) for Cr-30Co. It should be noted for future discussion that twins are not present in these alloys in the heat-treated condition.

Specimens were also examined metallographically after bend testing to study the mode of deformation. Photomicrographs of the Cr-Fe alloys after bend testing are shown in figures 8(a) to (c) for specimens annealed at 2300° F (1533° K) and quenched prior to bending. The initial mode of deformation for these alloys was primarily twinning. As the Fe content increased from 30 to 50 atomic percent, the number of twins decreased and the width of the twins increased. The maximum twin width was approximately 4.5×10^{-4} centimeter, which is in good agreement with the maximum twin width of 5×10^{-4} centimeter normally observed in body-centered cubic metals (ref. 17). These observations were also generally true as the solute content increased in Cr alloys with Co, Ru, and Re. However, twinning was not observed in the Cr-Os alloys which were two-phase above 12 atomic percent Os. Twinning also did not occur in unalloyed Cr or the less-concentrated alloys, for example, Cr-10Ru, as shown in figures 8(d) and (e), respectively.

A second feature evident in the Cr-Fe alloys is the substantial increase in grain size at a constant annealing temperature of 2300° F (1533° K) with increase in Fe content after reaching a minimum in grain size at an intermediate Fe content, figures 8(a) to (c). This

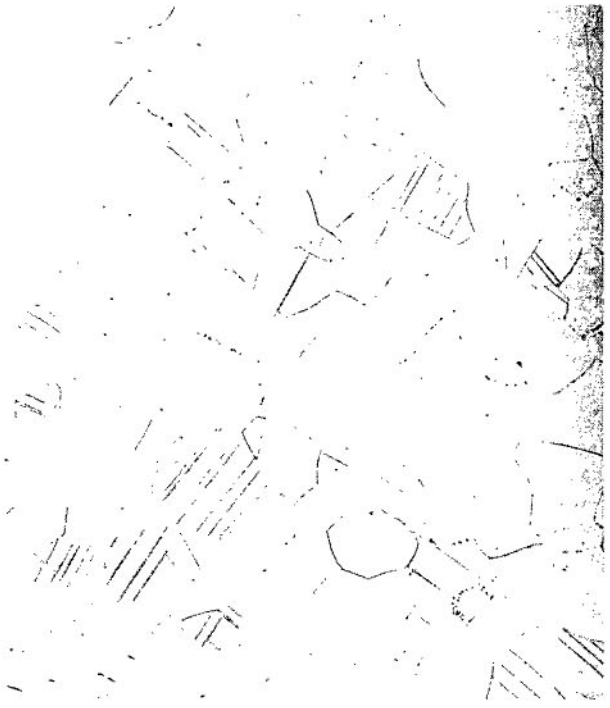

(a) Twins in Cr-35Fe.

(b) Twins in Cr-40Fe.

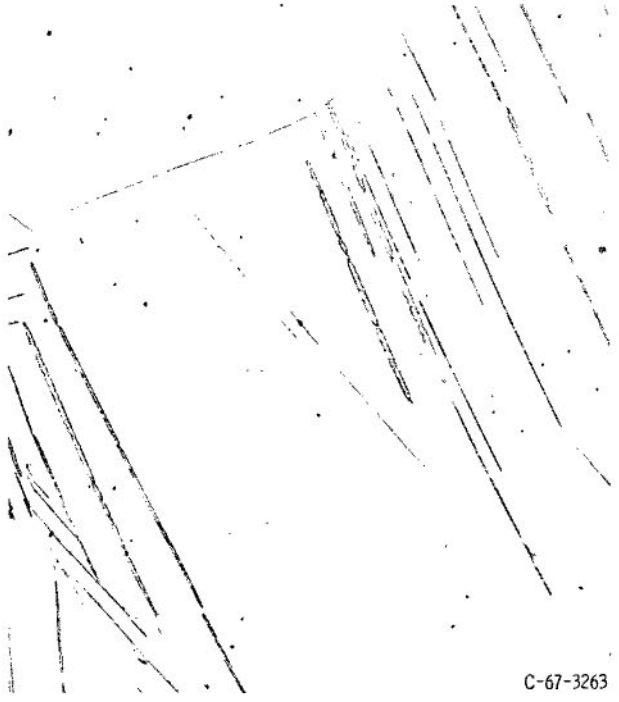

C-67-3263

(c) Twins in Cr-50Fe..

Figure 8. - Microstructures of deformed Cr-Fe, Cr-Ru, and unalloyed Cr. Specimens annealed and quenched prior to bend testing.

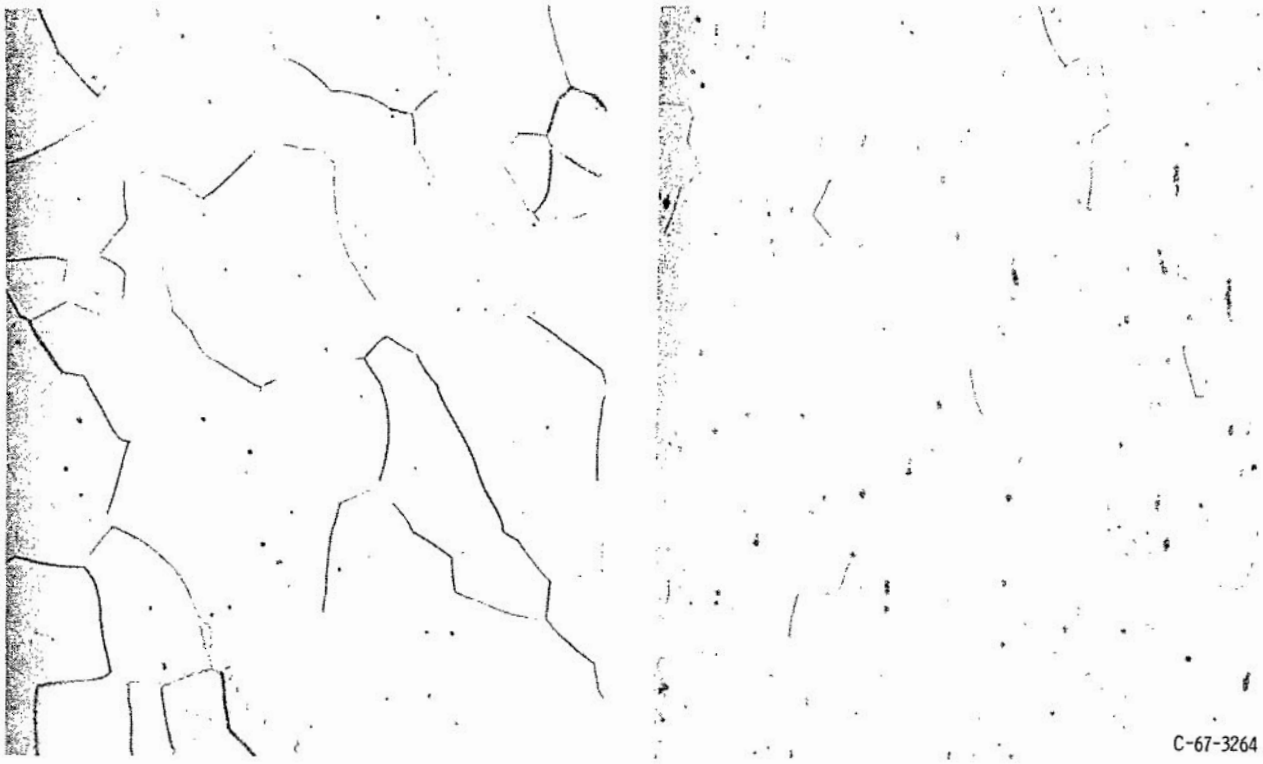

(d) Unalloyed Cr - no twins observed.

(e) Cr-10Ru - no twins observed.

Figure 8. - Concluded.

effect was also observed in the Cr-Co, Cr-Ru, and Cr-Re systems. The grain size data for these alloys are presented in table III and shown in figure 9. The increase in grain size ranges from 50 percent in Cr-Re to six-fold in Cr-Fe.

Bend Ductility

Results of bend tests conducted on quenched and furnace-cooled specimens are summarized in table III for the Cr-Re, Cr-Ru, Cr-Co, and Cr-Fe alloy systems. For the two alloy systems where the boundary is highly temperature dependent, Cr-Co and Cr-Fe (fig. 5), furnace cooling resulted in transition temperatures substantially higher than those of quenched specimens. This behavior was attributed to precipitation of σ during furnace cooling, shown in figure 7(b) for Cr-30Co. Alloys from systems in which the solvus line is less temperature dependent, Cr-Re and Cr-Ru (fig. 5), had comparable transition temperatures for the quenched and furnace-cooled conditions.

The effects of solute concentration on the ductile-to-brittle transition temperatures of quenched specimens from these four alloy systems are shown in figure 10. Dilute and intermediate alloy additions produced transition temperatures higher than that of unalloyed Cr. Alloying with 10 atomic percent Ru, for example, increased the transition tempera-

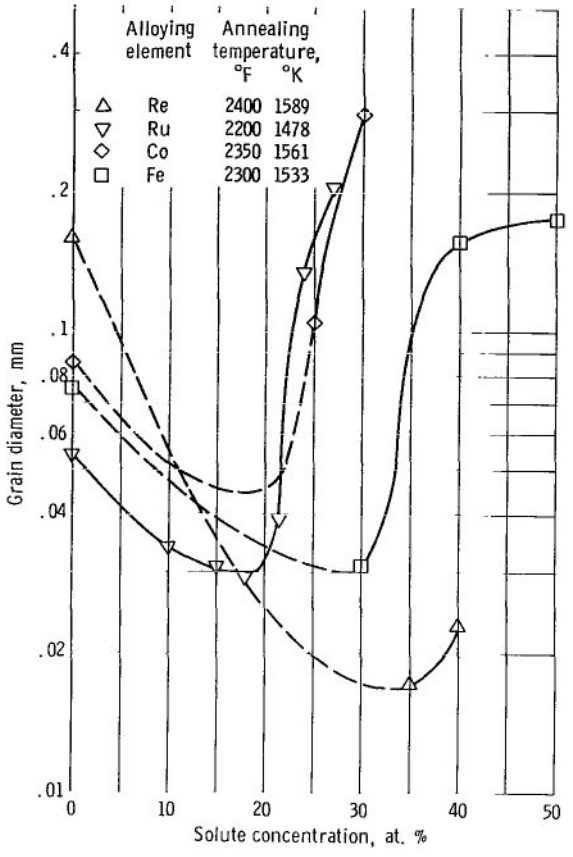

Figure 9. - Effect of solute concentration on grain size of Cr alloys. Annealed 1 hour at indicated temperatures; water quenched.

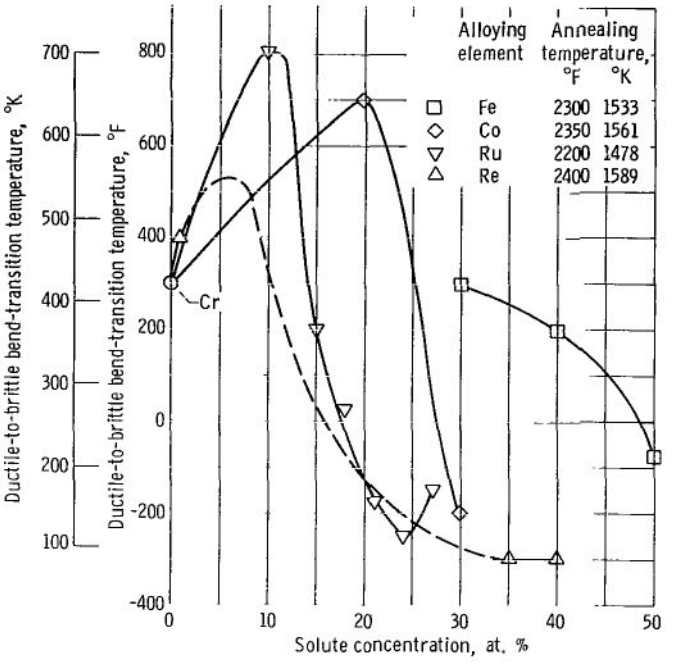

Figure 10. - Effect of solute concentration on ductile-to-brittle transition temperatures for chromium alloys. Annealed 1 hour at indicated temperatures; water quenched.

ture from 300° to 800° F (422° to 700° K), while the Cr-1.0Re had a transition temperature of 400° F (478° K). As the alloy composition approached the maximum solubility in Cr (Cr-Co, Cr-Ru, and Cr-Re systems) or the σ composition (Cr-Fe system), a sharp decrease in ductile-to-brittle transition temperature was observed. The transition temperatures ranged from -200° to -300° F (144° to 89° K) for the most ductile alloys containing Ru, Co, or Re, while a slightly higher transition temperature was observed for the most ductile Cr-Fe alloy, -75° F (214° K). An initial increase in transition temperature for Cr alloys containing up to 30 atomic percent Fe followed by a sharp decrease at concentrations up to 50 atomic percent Fe was reported previously (ref. 18).

Thus, another characteristic of alloys that exhibit the Re ductilizing effect, in addition to the high maximum solubility of solute in Cr and an intermediate σ phase, is that the lowest ductile-to-brittle transition temperatures are found in alloys having compositions near the maximum solubility of solute in Cr.

Two of the remaining seven systems which were investigated, Cr-Os and Cr-Mn,

also have phase diagrams similar to that of Cr-Re. Both have intermediate σ phases; Os has an estimated maximum solubility of 9.5 atomic percent in Cr, while Mn has a maximum solubility of 71 atomic percent.

Four alloys containing 6 to 15 atomic percent Os were fabricated as shown in table IV. The two alloys containing 12 and 15 atomic percent Os were hot rolled to good sheet, but the alloys containing 6 and 9 atomic percent Os were unfabricable. Bend-transition temperatures for the fabricable Cr-12Os and Cr-15Os alloys were 700° and 600° F, respectively, after annealing at 3000° F and quenching by withdrawing the specimens from the hot portion of the furnace and flowing Ar over them. Microstructural observations indicated that both of the annealed alloys were two phase the second phase presumably being σ.

However, recent information from C. S. Wukusick of General Electric suggests that Os (in Cr) may truly be another Re analogue. This information indicated that the cold fabricability of Cr-Os alloys increased with increasing solute content up to 22 atomic percent Os, and that the solubility of Os in Cr is 18 to 20 atomic percent at 2552° F (1673° K). Based on all of this information, it appears that the solubility of Os in Cr is highly temperature dependent, with a maximum solubility in the vicinity of 20 atomic percent, and that Os at sufficiently high levels may produce the Re ductilizing effect in Cr.

Three Cr-Mn alloys were prepared with solute contents of 35, 45, and 55 atomic percent Mn. However, as seen in table IV, all three alloys cracked on the first pass during attempted hot rolling. Thus, despite the phase similarities with Cr-Re, these data indicate that Mn is not a Re analogue in Cr.

Alloys were also investigated from six other Cr-base systems which have some similarities to the Cr-Re system, either a high solubility in Cr and/or a complex intermediate phase. These alloying elements included Cb, Ta, V, Ti, Ni, and Ir.

Columbium and Ta have low solubilities in Cr, but have a complex intermediate face-centered cubic phase (Cr-Cb) and a complex intermediate hexagonal close packed phase (Cr-Ta). Binary alloys containing 2.5 atomic percent Cb and 2.5 atomic percent Ta, near the solubility limits, were unfabricable.

Vanadium and Ti are completely soluble with Cr at elevated temperatures, with a low temperature hexagonal phase occurring in the Cr-Ti system. Three Cr-V alloys, containing 15, 30, and 45 atomic percent V, and a Cr-20Ti alloy were all unfabricable, as seen in table IV.

Nickel has a moderately high solubility in Cr, with no intermediate phase. An alloy containing 20 atomic percent Ni was unfabricable.

Finally, Ir forms two complex intermediate phases with Cr but has a low solubility in Cr, estimated at 2.5 atomic percent. A Cr-10Ir alloy was fabricable, but quenched specimens showed a bend-transition temperature of greater than 500° F (533° K).

It was originally postulated during this program that the importance of the σ phase might be associated with the difference in volume per atom between precipitating σ and solid solution, causing lattice strains and acting as dislocation sources. However, attempts to correlate the ductile-to-brittle transition temperature of the more ductile alloy in each system with the volume per atom difference between the σ phase and the saturated solid solution were unsuccessful.

Calculations based on specific volume, that is, considering the mass of the atoms, are presented in table V.

As shown in figure 11, a correlation does exist between ductile-to-brittle transition temperatures and differences in specific volume for the solid solutions and σ phases for the four alloys. Although the correlation shown may be fortuitous, the relation shown in figure 11 suggests that a metastable structure arising from quenching the alloys from near the solvus may be effective in lowering the ductile-to-brittle transition temperature. Straining the specimens during bending may cause precipitation of σ on a microscale or pre-precipitation during quenching may occur. For example, cold work has been shown to accelerate the formation of σ in a Cr-50Fe alloy, postulated to be due to stored strain energy from working being released by the transformation and making a large contribution to the driving force (ref. 19). It is suggested that the strains associated with σ phase nucleation can act as stress concentration sites to further nucleate dislocations and induce twinning. Apparently the greater the difference in specific volume ($1/\rho$) between the σ phase and the solid solution in which it is precipitating, the more effective the σ phase is as a dislocation source and the lower is the resulting ductile-to-brittle transition temperature. However, if σ precipitation occurs on a gross scale, the specimen then becomes embrittled.

TABLE V. - SPECIFIC VOLUMES OF SOLID SOLUTIONS AND σ PHASES FOR CHROMIUM ALLOYS

Solid solution composition, at. %	Specific volume of solid solution, cm^3g^{-1}	σ-Phase composition, at. %	Specific volume of σ phase, cm^3g^{-1}	Fractional difference in specific volume $\left(\frac{\text{Specific volume solid solution} - \text{Specific volume } \sigma}{\text{Specific volume solid solution}}\right)$
Cr-50Fe	0.133	Cr-57Fe	0.131	1.5×10^{-2}
Cr-30Co	.130	Cr-47Co	.126	3.1
Cr-24Ru	.122	Cr-33Ru	.111	9.0
Cr-35Re	.083	Cr-60Re	.062	25.3

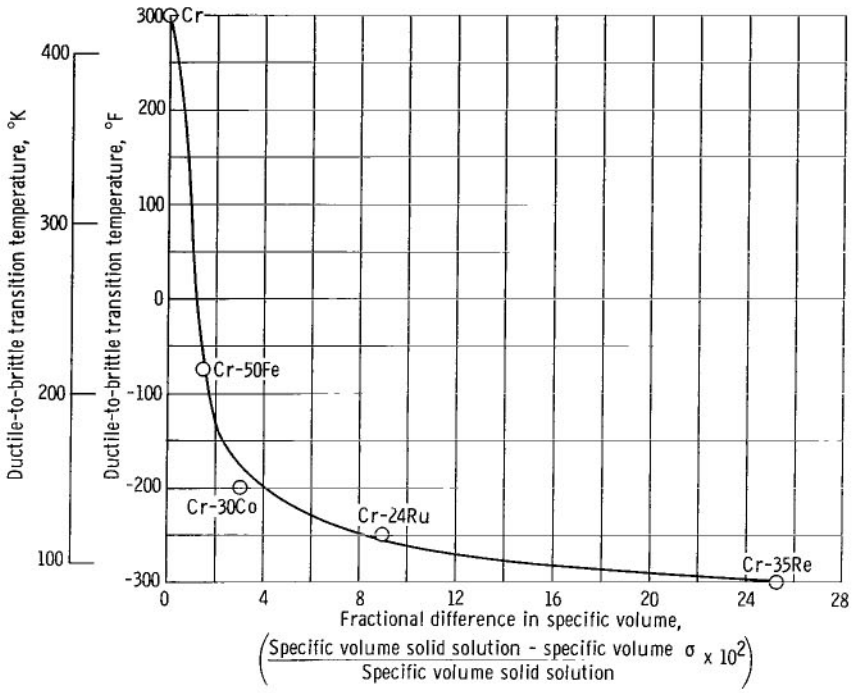

Figure 11. - Variation of transition temperature of Cr alloys with difference in specific volume of σ and solid-solution phases.

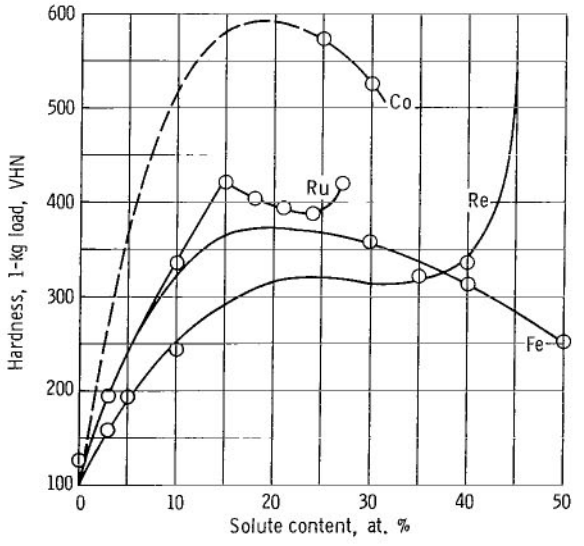

Figure 12. - Effect of solute concentration on room temperature hardness of Cr alloys. Shapes of Cr-Fe and Cr-Re curves based partly on data of Allen and Jaffee (ref. 2).

Hardness

Room temperature hardness determinations for the more concentrated alloys are presented in table III. These data are from specimens annealed at the constant temperature for each alloy system above the solvus temperature and then water quenched. Figure 12 combines the data for the dilute and intermediate alloy additions with the more concentrated additions for the Cr-Re, Cr-Ru, Cr-Co, and Cr-Fe systems and shows that after an initial hardness decrease, all four alloying elements increase the hardness substantially at intermediate alloying levels. However, the hardness decreases as the alloy composition approaches the maximum solubility in Cr for alloys with Re, Ru, and Co and the σ composition in the Cr-Fe system. The drop in hardness near the solubility limit for these alloy systems is consistent with hardness behavior reported for the Mo-Re and W-Re systems and provides further evidence that the same mechanism is operative in all six systems.

The hardness of the four alloy systems plus that for Cr-Os, Cr-Mn, and Cr-Ir are shown in figure 13 as a function of electron-to-atom ratio for each alloy composition. The data are seen to fit a smooth curve except where the drop in hardness occurs near the maximum solubility in Cr for six of the systems. The relation shown in figure 13 suggests that the number of free electrons per atom has a dominant effect on hardness of Cr alloys with elements from groups VII and VIII.

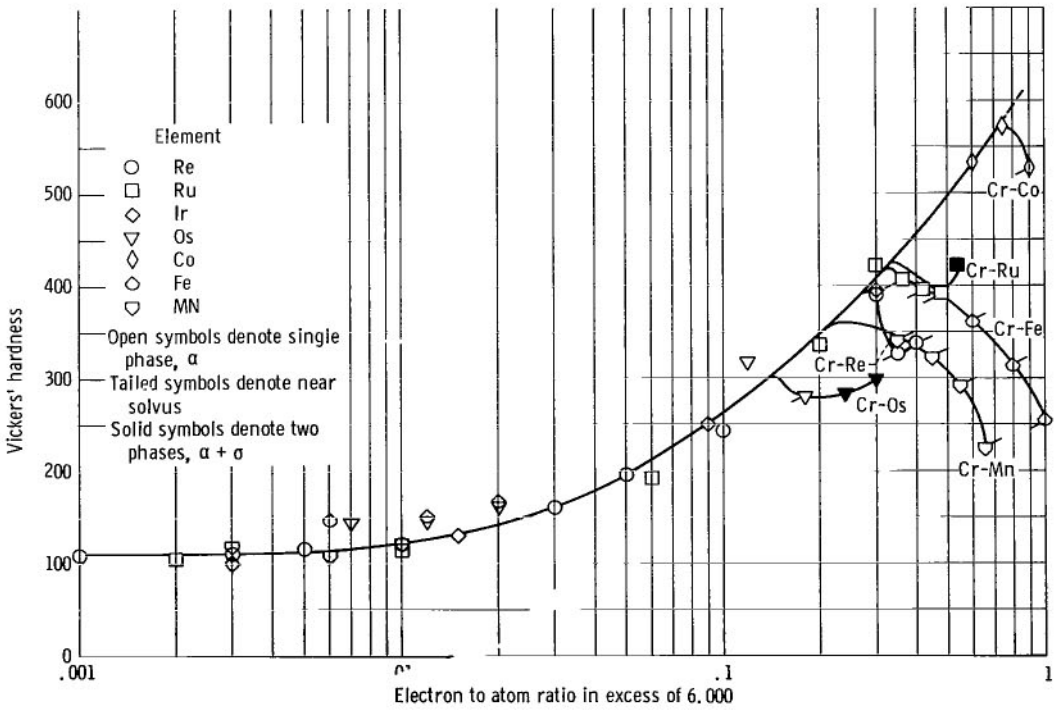

Figure 13. - Effect of electron per atom ratio on hardness of Cr alloyed with group VII and VIII elements.

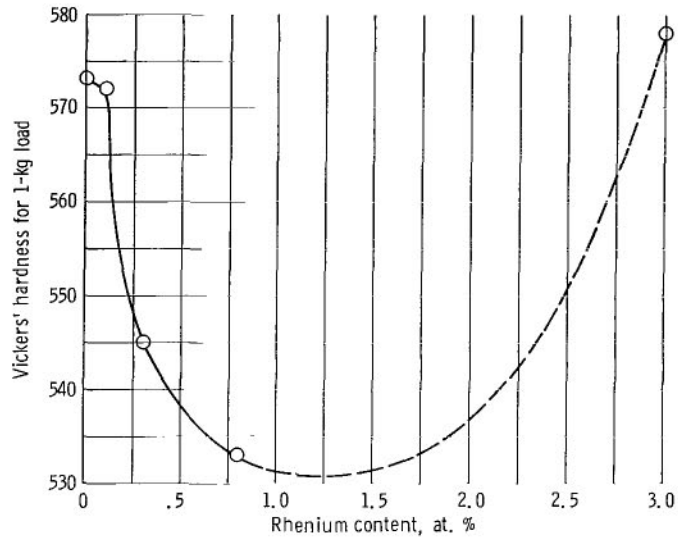

Figure 14. - Effect of rhenium content on room temperature hardness of as-cast Cr-30Co alloy.

Modification of Chromium-Rhenium and Chromium-Cobalt Alloys

Ternary alloys of Cr-Re-Co were investigated in an attempt to substitute Co for Re in the ductile high Re alloy. However, as shown in table IV, fabrication of alloys containing 10 to 30 atomic percent Re and 5 to 16 atomic percent Co was unsuccessful.

Ternary alloys of Cr - high Co - low Re were investigated to determine the effects of combining high Co ductilizing and softening by dilute Re additions. The Cr-30Co-0.1Re to Cr-30Co-3.0Re alloys, listed in table IV, appeared to be readily fabricable, and a reduction in hardness resulted with up to 0.8 atomic percent Re additions, as shown in figure 14. However, low loads encountered during bend testing and the high ductile-to-brittle transition temperatures, $\gtrsim 375^{\circ}$ F ($\gtrsim 464^{\circ}$ K), suggest that microcracks were produced during the rolling process.

Due to the large temperature dependence of the solubility limits in the Cr-Co system, alloys from this system are not useful for high-temperature application such as aircraft engine components since slow cooling from above the solvus results in precipitation of the embrittling σ phase. Ternary alloys of Cr-30Co-W, Cr-30Co-Mo, Cr-30Co-V, Cr-30Co-Ta, or Cr-30Co-Nb were investigated to determine the effects of these alloy additions on the solvus temperature. Hopefully, one or more ternary additions might reduce the tendency for σ precipitation, that is, lower the solvus temperature significantly.

Results of elevated temperature X-ray diffraction studies are presented in table VI. In most cases an increase in the ternary addition resulted in an increase in the solvus temperature. The largest increase was for the 4 atomic percent Mo alloy, where the

TABLE VI. - SOLVUS TEMPERATURES FOR CHROMIUM ALLOYS

Alloy composition, at. %	Transformation temperature	
	^{o}F	^{o}K
Cr-30Co[a]	2340	1555
Cr-30Co-2V[a]	2370	1570
Cr-30Co-4V[a]	2390	1580
Cr-30Co-6V[a]	2320	1545
Cr-30Co-1W[a]	2320	1545
Cr-30Co-2W[a]	2390	1580
Cr-30Co-4W[a]	2430	1605
Cr-30Co-1Mo[a]	2390	1580
Cr-30Co-2Mo[a]	2460	1620
Cr-30Co-4Mo[a]	2500	1645
Cr-2Ta-1Ta[b]	2370	1570
Cr-1Cb-4Ta[b]	2360	1565
Cr-2Cb-4Cb[b]	2340	1555

[a]Alloys were hot rolled at 2400° F (1589° K) to 0.03-in. (0.8 mm) sheet before grinding to powder.

[b]Unfabricable, no transformation temperature determined.

$\alpha/(\alpha + \sigma)$ transformation temperature was 2500° F (1644° K) compared to 2335° F (1553° K) for Cr-30Co. Fabrication of these alloys was successful; however, all alloys were brittle at room temperature, in the quenched condition.

Elevated Temperature Tensile Properties

Tensile properties for Cr-30Co and Cr-18, 21, 24, and 27 Ru are summarized in table VII. These data show that high elongation, characteristic of superplasticity, is found approximately near the solvus lines for the Cr-30Co alloy and the Cr-24Ru alloy.

For the Cr-30Co alloy (fig. 15), maximum elongation (160 percent) occurs just above the solvus temperature in the single-phase region and then decreases rapidly as the test temperature is increased or decreased.

Similar behavior was observed in the Cr-24Ru alloy where elongation was a maximum of 103 percent at a temperature just above the solvus, 2350° F (1561° K), and decreased

TABLE VII. - TENSILE PROPERTIES OF CHROMIUM-COBALT AND CHROMIUM-RUTHENIUM ALLOYS

Alloy composition, at. %	Annealed temperature		Test temperature		Elongation, percent	Upper yield stress[a]	
	^{o}F	^{o}K	^{o}F	^{o}K		lb/in.	N/m^2
Cr-30Co	2400	1589	[b]1900	1311	11	13 500	9.3×10^7
			[b]2100	1422	47	1 460	1.
			[b]2200	1478	86	790	.55
			2250	1505	160	1 000	.69
			2400	1589	125	500	.35
			2600	1700	42	140	.09
Cr-18Ru	2500	1644	1850	1283	14	16 800	12.4
Cr-18Ru			2200	1478	41	4 500	3.1
Cr-21Ru			1850	1283	17	15 500	10.7
			2200	1478	53	3 800	2.6
			2350	1561	66	2 200	1.5
			2500	1644	81	1 500	1.0
Cr-24Ru			1650	1172	25	24 100	16.6
			1850	1283	56	10 800	7.5
			2100	1422	78	4 500	3.1
			2200	1478	94	2 800	1.9
			2350	1561	103	1 800	1.2
			2500	1644	84	900	.6
Cr-27Ru			[a]1850	1283	36	8 400	5.8
			[a]2200	1478	69	3 200	2.2

[a]Upper yield stress and ultimate tensile stress are identical except for Cr-30Co tested at 1900^{o} and 2100^{o} F (1311^{o} and 1422^{o} K).

[b]Tested in $\alpha + \sigma$ region of equilibrium diagram.

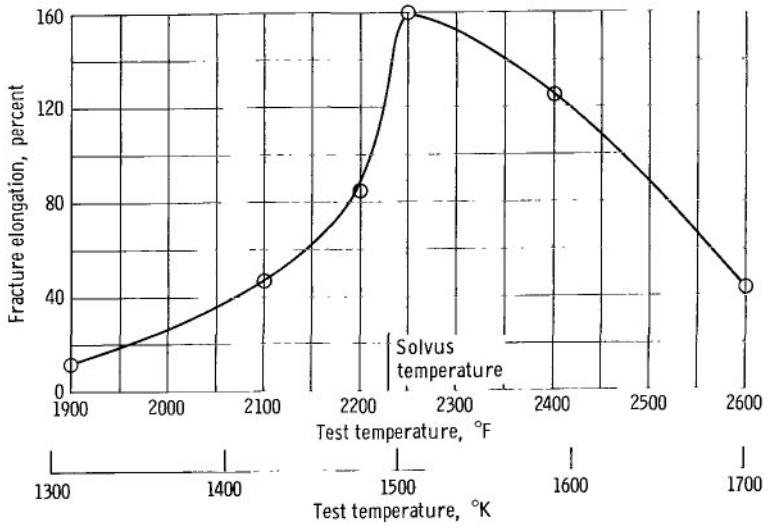

Figure 15. - Effect of test temperature on fracture ductility of a Cr-30Co alloy.

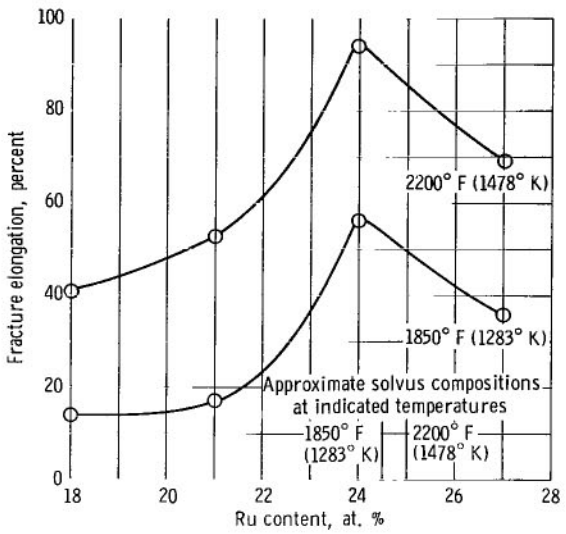

Figure 16. - Effect of Ru content on fracture ductility at 1850° and 2200° F (1283° and 1478° K).

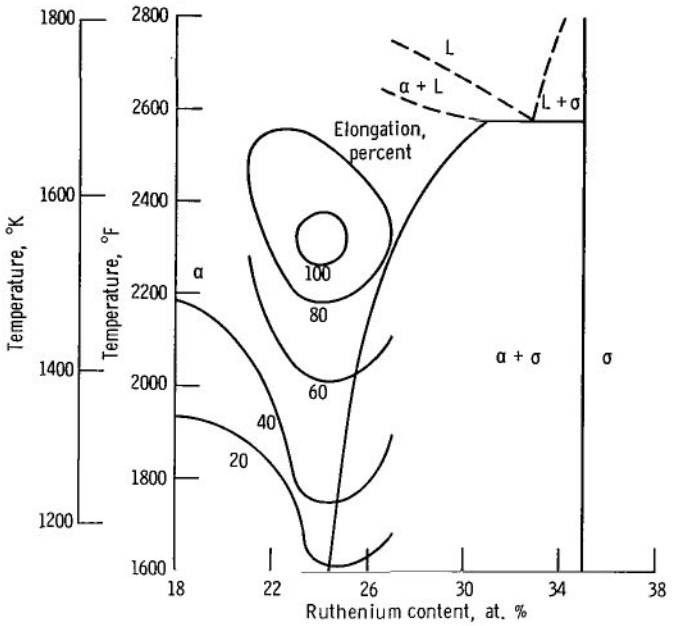

Figure 17. - Chromium-ruthenium system showing lines of constant elongation.

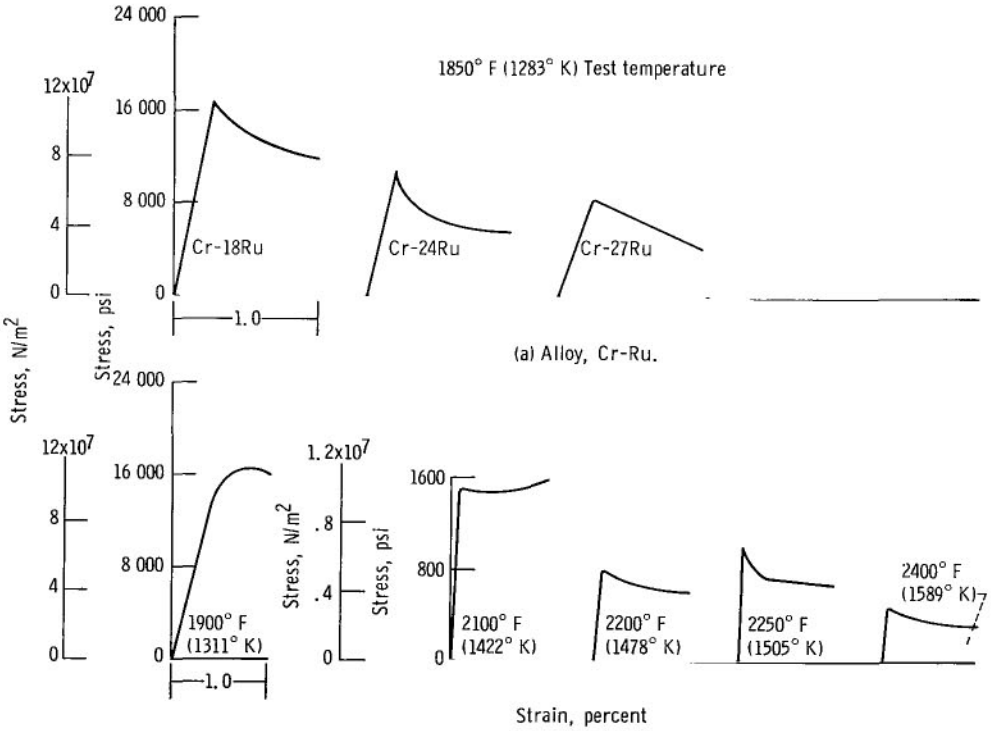

Figure 18. - Initial portion of stress-strain curves for Cr-Co and Cr-Ru alloys.

at higher or lower test temperatures. Figure 16 shows the change in elongation with increasing Ru content for alloys near the solvus composition at 1850° and 2200° F (1283° and 1478° K). Elongation is seen to increase with increasing Ru content up to the solvus composition and then decrease as the alloy becomes two phase. The elongation data for the Cr-Ru alloys are summarized in figure 17, where lines of constant elongation based on the measured elongations are superimposed on the partial equilibrium diagram. These data demonstrate the sharp increase in elongation in single-phase alloys near the solvus line.

Mechanical metastability near the solvus was also indicated in these alloys by their yielding and flow behavior. Figure 18(a) shows the stress-strain curves for three Cr-Ru alloys at 1850° F (1283° K). A sharp drop in stress occurs after yielding in these alloys: the largest decrease occurs in the Cr-24Ru, the composition nearest the solvus composition at the test temperature of 1850° F (1283° K). Similar behavior was observed in the Cr-30Co alloy at 2250° F (1505° K) just above the solvus temperature, as shown in figure 18(b). A sharp drop in stress occurred after yielding, but was less pronounced at test temperatures further removed from the solvus temperature. This type of yielding

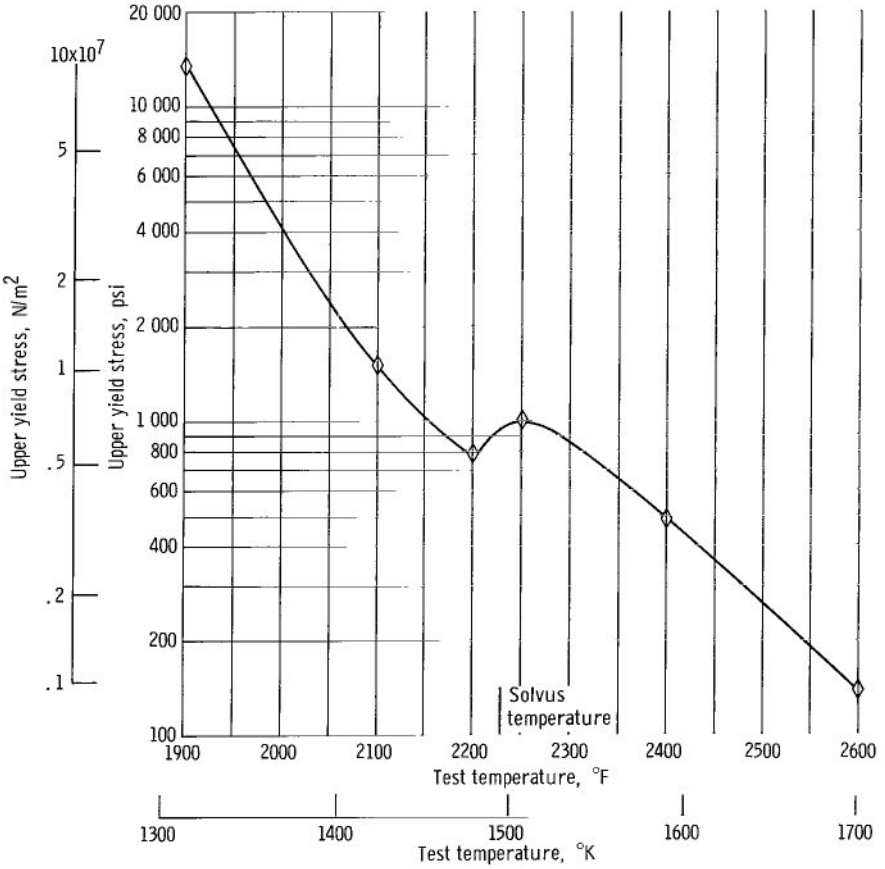

Figure 19. - Variation of upper yield stress of Cr-30Co with temperature tested in tension.

was also observed in W-24Re at 3500° F (2200° K) (ref. 5) and has been recently reported for a superplastic Ni-Fe-Cr alloy (ref. 20). Apparently, this yielding behavior indicates some type of resistance to flow which, when overcome, decreases in magnitude, analogous to stress-induced dislocation generation in the strain-aging temperature region.

Figures 19 and 20 show the upper yield stress as a function of temperature for the Cr-30Co alloy and as a function of Ru content at 2200° F (1478° K) in the Cr-Ru system, respectively. A discontinuity in upper yield stress curves exists as the solvus line is crossed.

Thus, superplasticity in these alloys is characterized by high, neck-free elongation, such as is observed in other superplastic alloys, for example, aluminum-zinc (Al-Zn) (ref. 21) and aluminum-copper (Al-Cu) (ref. 22). Superplasticity appears to be further characterized by a stress-strain curve that reaches a maximum stress at yielding and then gradually diminishes with additional deformation.

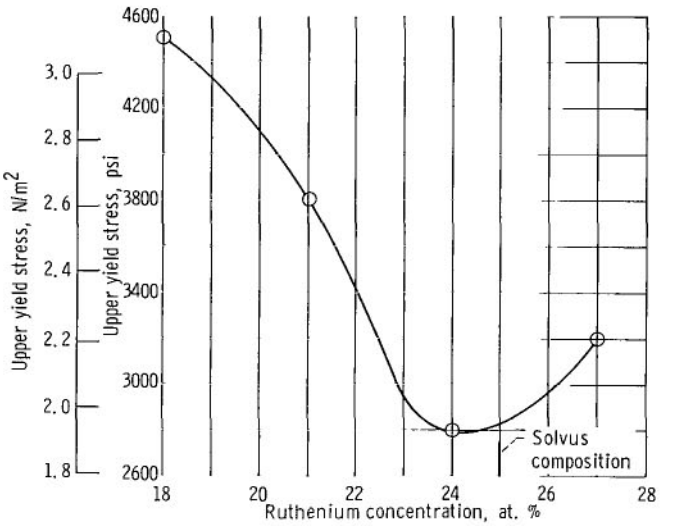

Figure 20. - Effect of solute concentration on upper yield stress of Cr-Ru alloys tested in tension at 2200° F (1478° K).

Discussion of the Rhenium Ductilizing Effect

The Re ductilizing effect on alloys of Re with Mo or W was first reported by Geach and Hughes (ref. 23). Since then, much effort has been expended to characterize the effect and several mechanisms have been suggested to explain the phenomenon. Review articles by Booth, et al. (ref. 6) and Gilbert, et al. (ref. 24) discuss the Re ductilizing effect and conclude that the mechanisms remain elusive. The mechanisms postulated by the authors of references 6 and 25 are the following:

(1) Rhenium changes the morphology of grain boundary oxide from a wetting type to a nonwetting type.

(2) Rhenium affects interstitial solubilities, either increasing, decreasing, or modifying precipitation kinetics (e.g., nitrides in Cr).

(3) Rhenium decreases the stacking fault energy and promotes twinning as an initial mode of deformation.

(4) Rhenium reduces the strain rate sensitivity, implying that cracks can be blunted by plastic deformation and the susceptibility to cleavage reduced.

(5) Rhenium changes the slip plane from {110} to {112}.

(6) Rhenium lowers the Peierls-Nabarro stress.

(7) Rhenium produces a critical electron-to-atom ratio; thus, Re optimizes ductility.

Many of these mechanisms undoubtedly contribute to the Re ductilizing effect; for example, twinning acts as a mode of deformation to relieve high localized stress, and evidence for lowering the Peierls-Nabarro stress was observed in W-2Re to W-9Re alloys but not in a W-24Re alloy (ref. 25). The reduction in strain rate sensitivity, permitting plastic flow rather than cleavage, also seems to be important.

The present investigation has characterized four Cr systems that exhibit the Re-ductilizing effect and several similarities of the systems appear to be important. These are an intermediate σ phase and a high solubility of the solute in Cr. Additionally, the composition of the most ductile alloy is near maximum solubility in the single-phase region. The mechanism by which these three factors contribute to reducing the ductile-to-brittle transition of Cr is postulated as follows:

(1) A high solubility and composition near maximum solubility favor a heterogeneous or segregated solid solution.

(2) During quenching or straining at lower temperatures, the metastable structure produces localized stresses and thus acts as dislocation and twin sources with a resulting lowering of the ductile-to-brittle transition temperature. We suggest that the increase in grain boundary mobility with increase in solute content up to the maximum solubility is evidence of solute segregation. Importance of the σ phase was suggested by the lower transition temperature with an increase in σ specific volume for the four alloy systems investigated.

Practically, these alloys are not promising as structural materials for such applications as stator vanes in proposed jet engines where typical 3000-hour rupture stresses of 4 ksi (2.8×10^7 N/m^2) at 2400° F (1589° K) or as turbine buckets where 3000-hour rupture stresses of 15 ksi (10.5×10^7 N/m^2) or higher at 2100° F (1422° K) are desired. The tensile strength of Cr-24Ru is only about 1.5 ksi (1.1×10^7 N/m^2) at 2400° F (1589° K). In contrast, unalloyed Cr and a Cr-4Mo-0.6Ta-0.4C-0.05Y have strengths of 2.6 ksi (1.8×10^7 N/m^2) and 20.4 ksi (14.3×10^7 N/m^2), respectively, at this temperature (data obtained from unpublished NASA Contract NAS 3-7260 with General Electric). In addi-

tion, Cr-35Re exhibits a 2400° F (1589° K) tensile strength of 22.3 ksi (15.6×10^7 N/m^2) (data obtained from unpublished NASA Contract NAS 3-7260 with General Electric); however, the high cost of Re is a serious deterrent to consideration of the alloy at this time.

CONCLUSIONS

An investigation of the low temperature mechanical properties and elevated temperature tensile properties of several Cr alloys led to the following conclusions:

1. Hardness minima in Cr containing dilute additions of groups VII and VIII elements are not associated with improved ductile-to-brittle bend-transition temperatures.

2. The Re ductilizing effect is observed in Cr alloys that have equilibrium diagrams similar to Cr-Re. Two important features of these diagrams, which include Cr-Fe, Cr-Co, and Cr-Ru as well as Cr-Re, are a high maximum solubility of solute in Cr and an intermediate σ phase.

3. It is postulated that the importance of the intermediate σ phase apparently arises from the quenched in metastable structure providing sites of high localized stresses which act as dislocation and twin sources.

4. Chromium alloys that exhibit the Re ductilizing effect are also superplastic, as shown for the Cr-Co and Cr-Ru alloy systems. These alloys also exhibit increased grain growth rates as compared to adjacent nonsuperplastic compositions.

Lewis Research Center,
National Aeronautics and Space Administration,
Cleveland, Ohio, September 12, 1967,
129-03-06-03-22.

REFERENCES

1. Sims, Chester T.: The Case for Chromium. J. Metals, vol. 15, no. 2, Feb. 1963, pp. 127-132.

2. Allen, B. C.; and Jaffee, R. I.: The Hardness Behavior of Chromium Alloyed with Group IV-A to VIII Transition Metals. Trans. ASM, vol. 56, no. 3, Sept. 1963, pp. 387-402.

3. Sherwood, L. L.; Schmidt, F. A.; and Carlson, O. N.: The Effect of Composition, Crystalline Condition and Thermal History on the Bend Transition Temperature of Chromium Alloys. Trans. ASM, vol. 58, no. 3, Sept. 1965, pp. 403-410.

4. Pugh, J. W.; Amra, L. H.; and Hurd, D. T.: Properties of Tungsten-Rhenium Lamp Wire. Trans. ASM, vol. 55, no. 3, Sept. 1962, pp. 451-461.

5. Klopp, William D.; Witzke, Walter R.; and Raffo, Peter L.: Mechanical Properties of Dilute Tungsten-Rhenium Alloys. NASA TN D-3483, 1966.

6. Booth, J. G.; Jaffee, R. I.; and Salkovitz, E. I.: The Mechanisms of the Rhenium-Alloying Effect in Group VI-A Metals. Metals for the Space Age. F. Benesovsky, ed., Metallwerk Plansee AG (Reutte, Austria), 1965, pp. 547-570.

7. Lawley, A.; and Maddin, R.: Tensile Behavior of Zone-Melted Molybdenum-Rhenium Single Crystals. Trans. AIME, vol. 224, no. 3, June, 1962, pp. 573-583.

8. Jaffee, R. I.; Maykuth, D. J.; and Douglass, R. W.: Rhenium and the Refractory Platinum-Group Metals. Refractory Metals and Alloys. M. Semchyshen and J. J. Harwood, eds., Interscience Publishers, 1961, pp. 383-463.

9. Wukusick, C. S.: The Rhenium Ductilizing Effect. Paper Presented at the AIME Conference on Physical Metallurgy of Refractory Metals, French Lick, Ind., Oct. 3-5, 1965.

10. Stephens, Joseph R.; and Klopp, William D.: Superplasticity and Low-Temperature Ductility in a Cr-30 At. Pct. Co Alloy. Trans. AIME, vol. 236, no. 11, Nov. 1966, pp. 1637-1639.

11. Klopp, William D; and Raffo, Peter L.: Effects of Purity and Structure on Recrystallization, Grain Growth, Ductility, Tensile, and Creep Properties of Arc-Melted Tungsten. NASA TN D-2503, 1964.

12. Wukusick, Carl S.: Research on Chromium-Base Alloys Exhibiting High-Temperature Strength, Low-Temperature Ductility, and Oxidation Resistance. (AF ASD-TDR-63-493), General Electric Co., June 1963.

13. Elliott, R. P.: Constitution of Binary Alloys. First Supplement. McGraw-Hill Book Co., Inc., 1965.

14. Wukusick, C. S.: Evaluation of Chromium-Ruthenium Alloys. Rep. No. GEMP-362, General Electric Co., June 25, 1965.

15. Hansen, Max: Constitution of Binary Alloys. McGraw-Hill Book Co., Inc., 1958.

16. Pearson, William B.: A Handbook of Lattice Spacings and Structures of Metals and Alloys. Pergammon Press, 1958.

17. Hull, D.: Growth of Twins and Associated Dislocation Phenomena. Deformation Twinning. R. E. Reed-Hill, J. P. Hirth, and H. C. Rogers, ed., Gordon and Breach Science Publishers, 1964, pp. 121-155.

18. Mil'man, Yu. V.; Rachek, A. P.; and Trefilov, V. I.: Mechanism of Deformation and Brittle Fractures of Transition Metals Alloys of Group VIa. Sb. Nauchn. Tr. Inst. Metallofiz. Akad. Nauk Ukr. SSR, no. 20, 1964, pp. 3-24.

19. Fisher, R. M.: The Role of Sub-Structure in Phase Transformations. Symposium on the Role of Substructure in the Mechanical Behavior of Metals. Rep. No. ASD-TDR-63-324, Aeronautical Systems Div., Wright-Patterson AFB, Apr. 1963, pp. 477-497.

20. Hayden, H. W.; Gibson, R. C.; Merrick, H. F.; and Brophy, J. H.: Superplasticity in the Ni-Fe-Cr System. Trans. ASM, vol. 60, no. 1, Mar. 1967, pp. 3-14.

21. Backofen, W. A.; Turner, I. R.; and Avery, D. H.: Superplasticity in an Al-Zn Alloy. Trans. ASM, vol. 57, no. 4, Dec. 1964, pp. 980-990.

22. Underwood, Ervin E.: A Review of Superplasticity and Related Phenomena. J. Metals, vol. 14, no. 12, Dec. 1962, pp. 914-919.

23. Geach, G. A.; and Hughes, J. E.: The Alloys of Rhenium with Molybdenum or with Tungsten and Having Good High-Temperature Properties. Plansee Proceedings, 1955. F. Benesovsky, ed., Pergamon Press, 1956, pp. 245-253.

24. Gilbert, A.; Klein, M. J.; and Edington, J. W.: Investigation of Mechanical Properties of Chromium, Chromium-Rhenium, and Derived Alloys. Battelle Memorial Inst. (NASA CR-81225), Aug. 31, 1966.

25. Stephens, J. R.: Transmission Microscopy Study of Deformation of Tungsten and Its Alloys. Paper Presented at the Fall Meeting of the AIME, Chicago, Ill., Oct. 30 to Nov. 3, 1966.

NASA-Langley, 1967 —— 14 E-3891

"The aeronautical and space activities of the United States shall be conducted so as to contribute . . . to the expansion of human knowledge of phenomena in the atmosphere and space. The Administration shall provide for the widest practicable and appropriate dissemination of information concerning its activities and the results thereof."

—NATIONAL AERONAUTICS AND SPACE ACT OF 1958

NASA SCIENTIFIC AND TECHNICAL PUBLICATIONS

TECHNICAL REPORTS: Scientific and technical information considered important, complete, and a lasting contribution to existing knowledge.

TECHNICAL NOTES: Information less broad in scope but nevertheless of importance as a contribution to existing knowledge.

TECHNICAL MEMORANDUMS: Information receiving limited distribution because of preliminary data, security classification, or other reasons.

CONTRACTOR REPORTS: Scientific and technical information generated under a NASA contract or grant and considered an important contribution to existing knowledge.

TECHNICAL TRANSLATIONS: Information published in a foreign language considered to merit NASA distribution in English.

SPECIAL PUBLICATIONS: Information derived from or of value to NASA activities. Publications include conference proceedings, monographs, data compilations, handbooks, sourcebooks, and special bibliographies.

TECHNOLOGY UTILIZATION PUBLICATIONS: Information on technology used by NASA that may be of particular interest in commercial and other non-aerospace applications. Publications include Tech Briefs, Technology Utilization Reports and Notes, and Technology Surveys.

Details on the availability of these publications may be obtained from:

SCIENTIFIC AND TECHNICAL INFORMATION DIVISION

NATIONAL AERONAUTICS AND SPACE ADMINISTRATION

Washington, D.C. 20546